UC Santa Barbara
UC Santa Barbara Previously Published Works

Title
Monolithic translucent BaMgAl10O17:Eu2+ phosphors for laser-driven solid state lighting

Permalink

Journal
AIP Advances, 6(10)

ISSN
2158-3226

Authors
Cozzan, Clayton
Brady, Michael J
OâDea, Nicholas
et al.

Publication Date
2016-10-01

DOI
10.1063/1.4964925

Peer reviewed

Monolithic translucent BaMgAl$_{10}$O$_{17}$:Eu^{2+} phosphors for laser-driven solid state lighting

Clayton Cozzan,[1, 2, 3] Michael J. Brady,[2] Nicholas O'Dea,[3] Emily E. Levin,[1, 2] Shuji Nakamura,[1, 3] Steven P. DenBaars,[1, 3] and Ram Seshadri[1, 2, 3, 4, a]

[1] *Materials Department, University of California, Santa Barbara, California 93106 USA*

[2] *Materials Research Laboratory, University of California, Santa Barbara, California 93106 USA*

[3] *Solid State Lighting and Energy Electronics Center, University of California, Santa Barbara, California 93106 USA*

[4] *Department of Chemistry and Biochemistry, University of California, Santa Barbara, California 93106 USA*

(Dated: 15 August 2016)

With high power light emitting diodes and laser diodes being explored for white light generation and visible light communication, thermally robust encapsulation schemes for color-converting inorganic phosphors are essential. In the current work, the canonical blue-emitting phosphor, high purity Eu-doped BaMgAl$_{10}$O$_{17}$, has been prepared using microwave-assisted heating (25 min) and densified into translucent ceramic phosphor monoliths using spark plasma sintering (30 min), both for the first time. The resulting translucent ceramic monoliths convert UV laser light to blue light with the same efficiency as the starting powder and provide superior thermal management versus silicone encapsulation.

Light emitting diode (LED)-based lighting is rapidly replacing incandescent and fluorescent sources,[1] and advances in semi-polar and non-polar substrates for LEDs have pushed current densities beyond 1000 A/cm^2.[2] Although current densities are increasing, laser diodes (LDs) have peak efficiencies at much higher operating currents than LEDs and therefore offer a higher power alternative to the droop-limited LEDs.[3] Currently, both LEDs and LDs are being explored for phosphor-converted white light, with LDs showing promise for high power white lighting.[4–6] Two common strategies are utilized for white light generation. Either a blue LED or LD is used in conjunction with a yellow-converting inorganic phosphor to generate a cool white light, or a near-UV/violet LED or LD is used to excite a mixture of blue, red, and green emitting inorganic phosphors to generate a warm white light.[7,8] Additionally, recent advances in laser diodes have also enabled promising data transmission rates for laser-based visible light communication,[9] with 2 Gbit/s demonstrated using a single crystal phosphor.[10] For these applications, more power in LDs means more flux than LED-based systems. Therefore, the high intensity light generated requires phosphor morphologies with high thermal conductivity to combat self-heating due to Stokes loss, which can both quench the phosphor and carbonize the silicone typically used for phosphor encapsulation.[11]

The current work focuses on both a fast way of preparing phosphor powders as well as a quick, encapsulation free scheme to prepare thermally robust phosphor monoliths suitable for high power LED- and LD-based applications. One way to make phase pure phosphors in a fast and energy efficient way is through microwave assisted heating. Eu-substituted BaMgAl$_{10}$O$_{17}$ (BAM:Eu^{2+}) was prepared by thoroughly mixing and grinding stoichiometric amounts of the starting materials BaCO$_3$ (99.999%, Sigma-Aldrich), MgO (99.95%, Cerac), Al$_2$O$_3$ (99.99%, Sigma-Aldrich), and Eu$_2$O$_3$ (99.99%, Sigma-Aldrich), which were pre-fired at 700 °C in a box furnace for 12 h. Samples containing 0.5 atom %, 1.0 atom %, 1.5 atom %, 2.0 atom %, 2.5 atom %, and 3.0 atom % europium substitution levels were prepared, *e.g.* the nominal composition for 1.5 atom % was Ba$_{0.985}$Eu$_{0.015}$MgAl$_{10}$O$_{17}$. LiF (99.995%, Aldrich) was added (2 wt %) as flux. The microwave heating procedure was based on prior work by Birkel *et al.*[12] For each preparation, 6 g of granular carbon (20 mesh from Sigma-Aldrich) was used as the microwave susceptor, and placed in a 20 mL alumina crucible (Advalue). Approximately 0.5 g of the unreacted sample powder was placed in a 5 mL alumina crucible, which was pushed into the carbon in the 20 mL crucible, covered with an alumina lid (Advalue), and placed in a block of high temperature alumina insulation foam. The materials were heated in a domestic microwave oven (Panasonic NN-SN667B, 1200 W) operating at 720 W for 25 min. This power and time were found to be highly reproducible and yielded the most efficient phosphors in this study. Other combinations of power and time produced the desired phase, but with phosphor efficiencies that were lower than that measured for samples prepared at 720 W for 25 min. This method is fast due to direct heating of the reactants, and reduces the reaction time of these samples by an order of magnitude.

To assess the phase purity of the microwave prepared phosphors, high resolution synchrotron powder diffraction data were collected using beamline 11 - BM at the Advanced Photon Source, Argonne National Laboratory using an average wavelength of 0.459266 Å. BAM:Eu^{2+} crystallizes in the hexagonal space group $P6_3/mmc$ (no. 194).[13,14] The refined structure was visualized using the open-source crystallographic software VESTA[15] and is

a)Electronic mail: seshadri@mrl.ucsb.edu

TABLE I. Unit cell data obtained from Rietveld refinements of X-ray synchrotron diffraction data. Numbers in parenthesis indicate the error in refined values.

a (Å)	5.623965(3)
b (Å)	5.623965
c (Å)	22.639717(22)
Cell volume (Å^3)	620.1360(10)
Space group	$P6_3/mmc$

shown in Fig. 1(a). The refined X-ray diffraction pattern for $Ba_{0.985}Eu_{0.015}MgAl_{10}O_{17}$ is shown in Fig. 1(b) with unit cell parameters shown in Table I. Rietveld refinements were performed using the General Structure Analysis System with EXPGUI.[16,17] No impurity phases were discovered or refined, and the R_{wp} of the fit was 11.75%. Ba and Eu occupancies were held constant at the nominal amounts. Peak shapes were handled using the pseudo-Voigt profile function, which combines Gaussian and Lorentzian components. The background was handled using a Chebyshev polynomial. The lack of impurities demonstrates the viability of microwave assisted heating for preparing phosphors.

For the next generation of LED and LD-based lighting, thermally robust phosphors are required. This can be achieved by avoiding low thermal conductivity encapsulating materials altogether and creating phosphor monoliths, such as single crystals or sintered ceramics. Once the desired phase has been prepared, spark plasma sintering (SPS) is one method to achieve stand-alone dense and robust ceramics in a technique that utilizes pressure and Joule heating. SPS can achieve near theoretical density in already prepared ceramic powders with certain crystal structures enabling translucency or transparency in oxides.[18] In cubic systems, such as the canonical yellow phosphor Ce-doped yttrium aluminum garnet, light scattering is dominated by pores, and the reduction of pores by optimizing SPS parameters and utilizing nanoparticulate starting materials results in transparent samples.[19–21] In hexagonal systems, such as BAM:Eu^{2+}, the refractive index is anisotropic and therefore depends on orientation of the grains. This anisotropy leads to additional grain scattering versus cubic crystals, making hexagonal systems, such as α-Al$_2$O$_3$, translucent at best and not transparent.[22]

In the present work, SPS was performed on already prepared BAM:Eu^{2+} powders using an FCT Systeme GmbH SPS furnace. Powders were placed in a graphite die of 10 mm diameter with 1 mm thick graphite foil. In SPS, the chamber holding the sample was pumped down to vacuum with a preload of 3 kN applied, and subsequently increased to 5 kN once vacuum was achieved. A heating rate of 200 °C was then initiated, the sample was heated to 1500 °C at a rate of 200 °C/min with a 5 min hold, and then finally cooled to room temperature in 10 min. The resulting monoliths were sanded to remove the graphite foil. The geometric density of
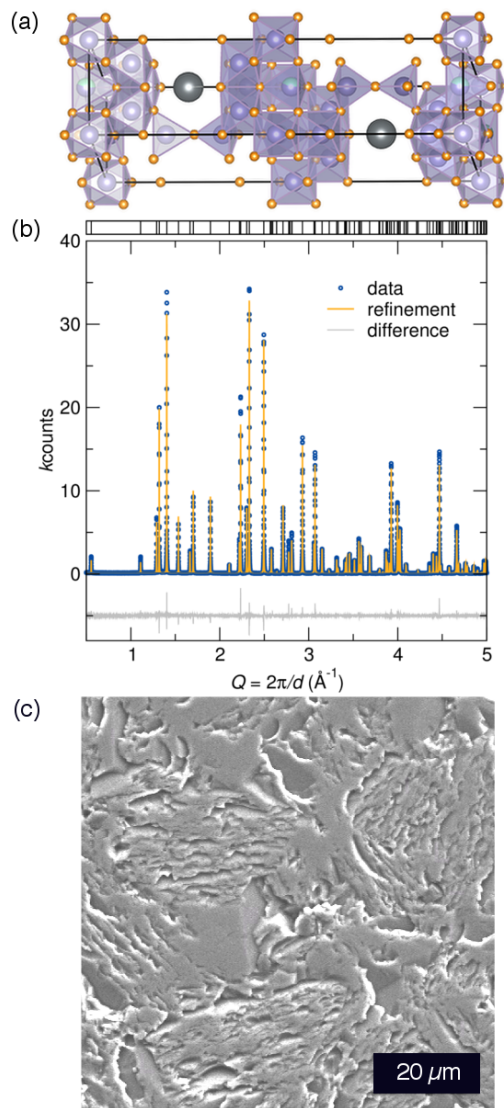

FIG. 1. (a) Hexagonal structure of $Ba_{0.985}Eu_{0.015}MgAl_{10}O_{17}$ shown with Ba atoms charcoal, O atoms orange, Al atoms green, Mg atoms purple, and Al/Mg-O polyhedra purple. (b) Synchrotron X-ray diffraction shows phase purity ($R_{wp} = 11.75\%$). (c) SEM micrograph of the BAM:Eu^{2+} dense monolith (black bar is 20 μm wide) shows the non-perfect arrangement of the hexagonal grains, leading to translucency and a density of 91.5%.

the SPS densified BAM:Eu^{2+} monolith was measured as 3.45 g/cm^3 ($\pm$ 0.05), which is 91.5% of the theoretical density of 3.770 g/cm^3 calculated from the refined unit cell of the starting powder. Scanning electron microscopy (SEM) images were collected on the monoliths using a FEI XL30 Sirion FEG Scanning Electron Microscope in secondary electron mode with a 15 kV beam voltage (Fig. 1(c)). There are regions of densely packed layers that are oriented in different angles relative to each other. This non-perfect stacking of hexagonal grains appears to create spacing in the stacks themselves, and is also likely the source of grain scattering that makes SPS-
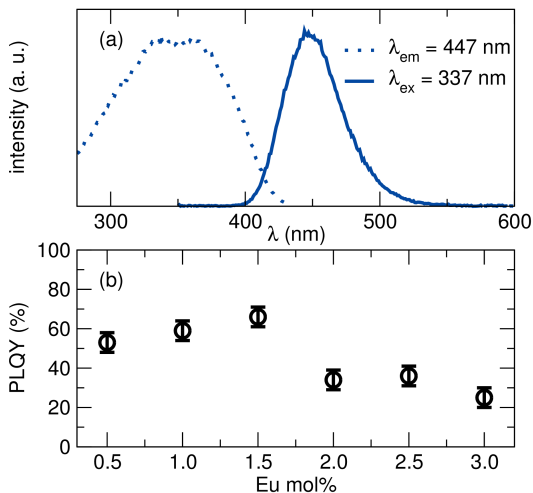
FIG. 2. (a) Excitation (dashed line) and emission (solid line) profiles of $Ba_{0.985}Eu_{0.015}MgAl_{10}O_{17}$ show strong absorption in the UV and blue emission due to the allowed $5d$ to $4f$ transition in Eu^{2+}. (b) QY as a function of Eu mol-% shows max QY $= 66\% \pm 5\%$ for 1.5 mol-% Eu nominally.

FIG. 3. Photograph of (a) translucent $BAM:Eu^{2+}$ monolith held by carbon-tipped tweezers and (b) excited by a 402 nm laser diode incident perpendicular to the surface of the monolith. Under violet laser excitation, the phosphor powder in silicone (c) exceeded 360 °C and carbonized in 11 s, whereas the translucent sample (d) only reached 70 °C. White lines on color bar mark 100 °C increments.

prepared monoliths of this material translucent and not transparent, as well as the measured density of 91.5%.

Room temperature photoluminescence spectra and quantum yield (QY) on the initial $BAM:Eu^{2+}$ powder were measured using a fluorescence spectrometer (Horiba, Fluoromax 4) and are shown in Fig. 2(a) and Fig. 2(b), respectively. $BAM:Eu^{2+}$ shows strong absorption in the UV and emission centered around 445 nm (Fig. 2(a)). The emission is due to the excited $4f^6 5d$ relaxing to the $4d^6$ ground state.[13] No emission is observed around 600 nm, which confirms the presence of Eu^{2+} in the lattice instead of Eu^{3+}, demonstrating the versatility of microwave assisted heating for preparing phosphor samples. QY of the starting powder was measured as a function of Eu mol% (Fig. 2(b)). The maximum QY of 66 % (± 5 %) for $\lambda_{ex} = 340$ nm was achieved for the 1.5 mol % sample. The Commission Internationale de l'Éclairage (CIE) 1931 (x, y) coordinates were $(0.15, 0.05)$ for all samples measured. Phosphors were thoroughly mixed by 25-wt % in a silicone matrix (Momentive, RTV-615) using a high speed mixing system (FlackTek Inc., DAC 150.1 FVZ-K) at 1500 rpm for 5 min, and subsequently deposited on a fused silica substrate (Chemglass) and cured at 105 °C for 15 min in a box oven. Phosphors encapsulated in a silicone matrix were then placed in a 15 cm diameter, Spectralon®-coated integrating sphere (Horiba, Quanta-ϕ) and excited by 340 nm light, which was generated by a 150 W continuous output, ozone-free xenon lamp. QY was calculated based on the work by de Mello *et al.*[23]

To demonstrate viability of the phosphor monoliths with a LD, QY was calculated using a 50 cm diameter integrating sphere with a commercial laser mounted in a side port and the phosphor sample mounted in the center of the sphere. The QY ($\lambda_{ex} = 400$ nm) using a fluorimeter
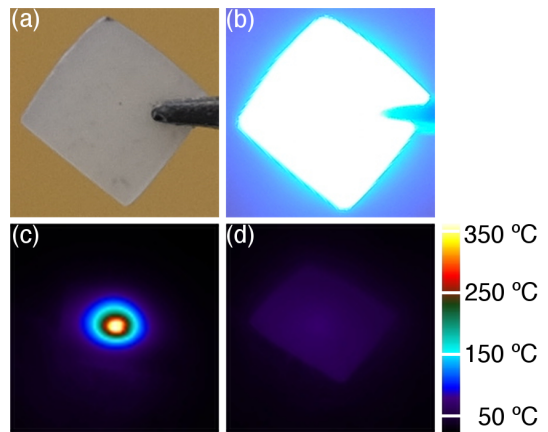
of the phase pure starting powder encapsulated in silicone was $33\% \pm 5$ %. The same QY within error ($37\% \pm 5$ %) was calculated for the translucent ceramic monolith using both a LD and a fluorimeter, indicating that densification of the $BAM:Eu^{2+}$ powder into a translucent monolith does not lower the QY. Photographs of a $BAM:Eu^{2+}$ sample without and with a commercial violet LD incident to its surface are shown in Fig. 3(a) and (b), respectively. For QY measurements with a LD, the monolith surface was positioned at a slight angle from the incoming laser beam to prevent reflection back towards the laser port, and the distance between the laser and the sample was 30 cm. The commercially available laser diode, with λ_{max} = 402 nm, FWHM = 2.6 nm, threshold current of 30 mA, and wall plug efficiency (WPE) of 20%, was mounted in a copper heat sink. The diode was operated at 500 mA with a voltage of 6.11 V (595 mW of laser power in output light incident on sample surface) controlled by a Keithley 2440 5A SourceMeter. The laser was observed to redshift with increasing current, registering 406 nm at 500 mA.

To study the thermal management of a translucent ceramic monolith versus phosphor powder in silicon, commercial $BAM:Eu^{2+}$ powder encapsulated in silicone (25 wt% phosphor) and a translucent ceramic monolith prepared using the same commercial powder were thermally isolated on quartz wool, irradiated with a laser diode placed 5 cm from the sample surface, and monitored using a FLIR A310 thermal imaging camera (range 0 °C–360 °C). After 11 s of laser irradiation, the phosphor powder in silicone (Fig. 3(c)) exceeded 360 °C and carbonized. In the same time, the translucent ceramic (Fig. 3(d)) reached 70 °C. After two minutes of laser irradiation, the translucent sample reached 160 °C. Both samples had the same dimensions (6 mm x 6 mm x 1 mm), and the laser diode was operated at the same current

and voltage as the QY measurements (595 mW of optical power incident on the sample). The superior thermal management observed shows promise for BAM:Eu^{2+} ceramic monoliths as a blue component in LED- and LD-based lighting.

In summary, phosphor powders were prepared using microwave-assisted heating in 25 min, which reduces preparation time and energy consumption. Results of the refinement on synchrotron X-ray diffraction data demonstrate the viability of microwave assisted heating for preparing phase pure BAM:Eu^{2+}. Phosphor powders can be densified into translucent and dense ceramic monoliths using SPS in only 30 min, which offers a fast way to produce encapsulation-free phosphors. QY of the starting powder does not change after densification into a translucent monolith. Due to the monolithic nature of the present blue-emitting phosphor, translucent phosphors prepared in this way mitigate phosphor self-heating greatly as compared to silicone encapsulation, making them extremely useful as a UV light filter and/or a blue component in warm white light generation using near-UV LEDs and LDs for general illumination and visible light communication.

[1] J. Brodrick, "Energy savings forecast of solid-state lighting in general illumination applications," Tech. Rep. (US Dep. Energy, Washington DC, 2014).

[2] S. Nakamura and M. R. Krames, "History of gallium–nitride-based light-emitting diodes for illumination," Proc. IEEE **101**, 2211–2220 (2013).

[3] L. Y. Kuritzky and J. S. Speck, "Lighting for the 21st century with laser diodes based on non-basal plane orientations of GaN," MRS Commun. **5**, 463–473 (2015).

[4] K. A. Denault, M. Cantore, S. Nakamura, S. P. DenBaars, and R. Seshadri, "Efficient and stable laser-driven white lighting," AIP Adv. **3**, 072107 (2013).

[5] Q.-Q. Zhu, X.-J. Wang, L. Wang, N. Hirosaki, T. Nishimura, Z.-F. Tian, Q. Li, Y.-Z. Xu, X. Xu, and R.-J. Xie, "β-Sialon:Eu Phosphor-in-Glass: a Robust Green Color Converter for High Power Blue Laser Lighting," J. Mater. Chem. C **3**, 10761–10766 (2015).

[6] M. Cantore, N. Pfaff, R. M. Farrell, J. S. Speck, S. Nakamura, and S. P. DenBaars, "High luminous flux from single crystal phosphor-converted laser-based white lighting system," Opt. Express **24**, A215–A221 (2016).

[7] N. C. George, K. A. Denault, and R. Seshadri, "Phosphors for Solid-State White Lighting," Annu. Rev. Mater. Res. **43**, 481–501 (2013).

[8] J. Sheu, S. Chang, C. Kuo, Y. Su, L. Wu, Y. Lin, W. Lai, J. Tsai, G. Chi, and R. Wu, "White-Light Emission from Near UV InGaN-GaN LED Chip Precoated with Blue/Green/Red Phosphors," IEEE Photon. Technol. Lett. **15**, 18–20 (2003).

[9] C. Lee, C. Zhang, M. Cantore, R. M. Farrell, S. H. Oh, T. Margalith, J. S. Speck, S. Nakamura, J. E. Bowers, and S. P. DenBaars, "4 Gbps direct modulation of 450 nm GaN laser for high-speed visible light communication," Opt. Express **23**, 16232–16237 (2015).

[10] C. Lee, C. Shen, H. M. Oubei, M. Cantore, B. Janjua, T. K. Ng, R. M. Farrell, M. M. El-Desouki, J. S. Speck, S. Nakamura, *et al.*, "2 Gbit/s data transmission from an unfiltered laser-based phosphor-converted white lighting communication system," Opt. Express **23**, 29779–29787 (2015).

[11] X. Luo, X. Fu, F. Chen, and H. Zheng, "Phosphor self-heating in phosphor converted light emitting diode packaging," International Journal of Heat and Mass Transfer **58**, 276–281 (2013).

[12] A. Birkel, K. A. Denault, N. C. George, C. E. Doll, B. Hery, A. A. Mikhailovsky, C. S. Birkel, B.-C. Hong, and R. Seshadri, "Rapid microwave preparation of highly efficient Ce^{3+}-substituted garnet phosphors for solid state white lighting," Chem. Mater. **24**, 1198–1204 (2012).

[13] Y.-I. Kim, K.-B. Kim, M.-J. Jung, and J.-S. Hong, "Combined rietveld refinement of $BaMgAl_{10}O_{17}$:Eu^{2+} using X-ray and neutron powder diffraction data," J. Lumin. **99**, 91–100 (2002).

[14] K.-B. Kim, Y.-I. Kim, H.-G. Chun, T.-Y. Cho, J.-S. Jung, and J.-G. Kang, "Structural and optical properties of $BaMgAl_{10}O_{17}$:Eu^{2+} phosphor," Chem. Mater. **14**, 5045–5052 (2002).

[15] K. Momma and F. Izumi, "VESTA: a Three-Dimensional Visualization System for Electronic and Structural Analysis," J. Appl. Crystallogr. **41**, 653–658 (2008).

[16] A. C. Larson and R. B. Von Dreele, "GSAS," General Structure Analysis System. LANSCE, MS-H805, Los Alamos, New Mexico (1994).

[17] B. H. Toby, "EXPGUI, a Graphical User Interface for GSAS," J. Appl. Crystallogr. **34**, 210–213 (2001).

[18] J. Garay, "Current-activated, pressure-assisted densification of materials," Annu. Rev. Mater. Res. **40**, 445–468 (2010).

[19] R. Chaim, R. Marder-Jaeckel, and J. Shen, "Transparent YAG ceramics by surface softening of nanoparticles in spark plasma sintering," Mat. Sci. Eng. A-Struct. **429**, 74–78 (2006).

[20] R. Chaim, M. Kalina, and J. Z. Shen, "Transparent yttrium aluminum garnet (YAG) ceramics by spark plasma sintering," J. Eur. Ceram. Soc. **27**, 3331–3337 (2007).

[21] N. Frage, S. Kalabukhov, N. Sverdlov, V. Ezersky, and M. P. Dariel, "Densification of transparent yttrium aluminum garnet (YAG) by SPS processing," J. Eur. Ceram. Soc. **30**, 3331–3337 (2010).

[22] R. T. Marta Suárez, Adolfo Fernández and J. L. Menendez, *Sintering to Transparency of Polycrystalline Ceramic Materials* (InTech Open Access Publisher, 2012).

[23] J. C. de Mello, H. F. Wittmann, and R. H. Friend, "An improved experimental determination of external photoluminescence quantum efficiency," Adv. Mater. **9**, 230–232 (1997).